ACS APPLIED MATERIALS & INTERFACES

Research Article

www.acsami.org

High-Concentration Synthesis of Sub-10-nm Copper Nanoparticles for Application to Conductive Nanoinks

Yuki Hokita, Mai Kanzaki, Tomonori Sugiyama, Ryuichi Arakawa, and Hideya Kawasaki*

Faculty of Chemistry, Materials and Bioengineering, Kansai University, 3-3-35 Yamate-cho, Suita 564-8680, Japan

Supporting Information

ABSTRACT: A simple, high-concentration (up to 0.6 M Cu salt) synthesis of sub-10-nm copper nanoparticles (Cu NPs) was developed in ethylene glycol at room temperature under ambient air conditions using 1-amino-2-propanol (AmIP) as the stabilizer. Monodispersed AmIP-Cu NPs of 3.5 ± 1.0 nm were synthesized in a high yield of ∼90%. Thus, nearly 1 g of sub-10-nm Cu NP powder was obtained using a one-step synthesis for the first time. It is proposed that metallacyclic coordination stability of a five-membered ring type between the Cu and AmIP causes the high binding force of Am IP onto the Cu surface, resulting in the superior stability of the AmIP-Cu NPs in a solution. The purified powder of AmIP-Cu NPs can be redispersed in alcohol-based solvents up to high Cu contents of 45 wt % for the preparation of Cu nanoink. The resistivity of the conductive Cu film obtained from the Cu nanoink was 30 μΩ cm after thermal heating at 150 °C for 15 min under a nitrogen flow. The long-term resistance stability of the Cu film under an air atmosphere was also demonstrated.

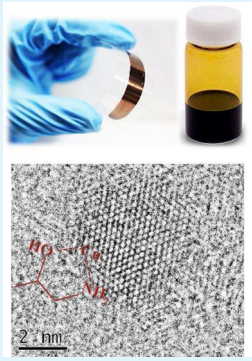

KEYWORDS: *copper nanoparticles, sub-10-nm, cu nanoink, solution synthesis, low-temperature sintering, alcohol-based solvents*

1. INTRODUCTION

Owing to their outstanding thermal conductivity, electrical conductivity, and chemical and optical properties, copper nanoparticles (Cu NPs) have been used for many purposes such as conductive nanoink,[1] optical nanodevices,[2] catalysts,[3] and antibacterial agents.[4] Among such applications, Cu NP conductive nanoinks have received growing interest in relation to printable electronics on plastic substrates.[5] Most of the recent studies on conductive nanoinks have focused on silver nanoparticles because of their high conductivity and oxidation resistance.[6−9] However, silver metals are too expensive to be used in large quantities. Furthermore, silver electrical circuits often suffer the problem of electro-migration. Therefore, Cu NPs are considered an alternative for conductive nanoinks because of their high conductivity, low cost, and reduced electro-migration effect.[10−20] At present, the major problem associated with Cu NPs is their low oxidation resistance in ambient air conditions;[21−23] the presence of copper oxide not only raises the sintering temperature but also dramatically reduces the electrical conductivity of Cu NPs (i.e., 5.1×10^{7} Ω cm for CuO and 1.7×10^{-6} Ω cm for Cu).

Since the melting temperature of Cu NPs decreases with their size reduction, notably in the single nanosized sub-10-nm Cu NPs, several approaches for the fabrication of Cu nanoink have been developed for the solution-based synthesis of sub-10 nm Cu NPs via the chemical reduction of copper(II) salts in the presence of organic stabilizers.[22,24−34] However, two major issues are encountered in the solution synthesis of sub-10 nm Cu NPs. One issue is that the use of strongly bonded organic stabilizers, such as surfactants and polymers, is essential during the synthesis to avoid the oxidation and aggregation of the Cu NPs.[22,24−34] However, the organic stabilizers act as insulating organic shells around each particle surface after the thermal sintering of Cu nanoink at heating temperatures of less than 150 °C; this prevents electrical conductivity in the Cu film. The other issue is the use of a low concentration of Cu(II) salts (typically <50 mM) during the solution synthesis of sub-10-nm Cu NPs to avoid the aggregation of small particles or their growth into larger particles, since high-concentration synthesis of Cu NPs is desirable for the preparation of high-concentration Cu nanoink (typically more than 20 wt % Cu) in large quantities. Usually, to achieve high-concentration synthesis (>100 mM) of Cu NPs, strongly bonded organic stabilizers are needed to avoid the aggregation.[10,24] However, the organic stabilizers prevent electrical conductivity in the Cu film. Therefore, the use of strongly bonded organic stabilizers is a trade-off between high-concentration synthesis of stable sub-10-nm Cu NPs and the undesirable presence of insulating organic stabilizers after thermal sintering of Cu nanoink. Due to this trade-off issue, the high-concentration (>300 mM) solution synthesis of sub-10-nm Cu NPs and its application to the production of conductive Cu nanoink have not yet been reported.

In this study, we first demonstrated the high-concentration (up to 0.6 M) solution synthesis of Cu NPs with a narrow size distribution of 3.5 ± 1.0 nm in ethylene glycol under ambient air conditions using 1-amino-2-propanol (AmIP) as a capping agent of low molecular weight, M = 75.1. The AmIP-protected Cu NP (AmIP-Cu NP) powders could be separated by adding poor solvent from the as-prepared colloidal Cu solution, and

Received: June 22, 2015
Accepted: August 13, 2015
Published: August 19, 2015

DOI: 10.1021/acsami.5b05542
ACS Appl. Mater. Interfaces 2015, 7, 19382−19389

Scheme 1. Schematic Illustrating the Synthesis of AmIP-Cu NPs and the Preparation of AmIP-Cu NP-Based Ink

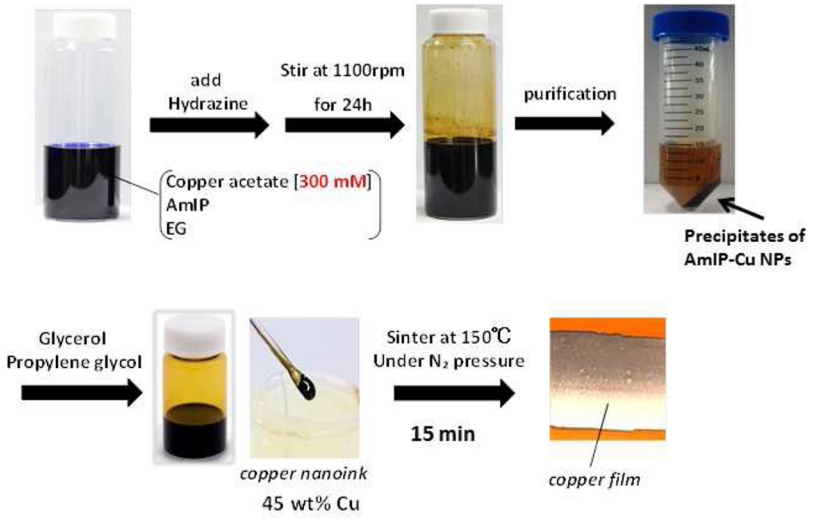

nearly 1 g of sub-10-nm Cu NP powder was obtained in this one-step synthesis. The AmIP-Cu NP powders had very high Cu content (~90 wt %), and they were well-dispersed in an alcohol-based ink up to 45 wt %. The antioxidative conductive copper films were obtained from the AmIP-Cu NP-based nanoink after thermal sintering at 150 °C for a short period of 15 min under a N_2 atmosphere, resulting in low electrical resistivity of 30 $\mu\Omega$ cm. In relation to the potential application of the AmIP-Cu NP-based nanoink in the printed electronics industry, the long-term resistance stability of Cu film under an air atmosphere was determined, and an adhesion test on polyethyleneterephthalate (PET) film was also conducted.

2. EXPERIMENTAL SECTION

2.1. Materials. All the chemicals were used as received without further purification. The 1-amino-2-propanol (AmIP, 98.0%), 3-amino-1-propanol (AmNP, 98.0%), copper(II) acetate anhydrate (97.0%), copper(II) formate (98%), copper(I) oxide powder, propylene glycol (99.0%), ethylene glycol (99.5%), ethanol (99.5%), hydrazine monohydrate (98.0%), *N,N*-dimethylacetamide (98.0%), toluene (98.0%), and hexane (96.0%) were purchased from Wako Chemicals, Japan.

2.2. Synthesis of AmIP-Cu NPs and Preparation of AmIP-Cu NP-Based Ink. The solution synthesis of AmIP-Cu NPs and the preparation of AmIP-Cu NP-based ink are summarized in Scheme 1.

Synthesis. The AmIP-Cu NPs were synthesized in ethylene glycol with a high concentration of copper(II) acetate under ambient air conditions at room temperature using AmIP as the stabilizer and hydrazine monohydrate as the reducing agent (molar ratio of Cu salt/AmIP/hydrazine = 1:10:10). Typically, 11 mL of AmIP was added to 30 mL of ethylene glycol. Solid copper(II) acetate (2.73 g) was added into the AmIP solution in an ice bath, producing a blue solution due to the formation of an AmIP-Cu complex. This solution had a concentration of 300 mM Cu salt. Then, hydrazine monohydrate (7.3 mL) was added all at once, under stirring at 1100 rpm and at room temperature (~23 °C), to the blue solution. The color of the resulting solution rapidly changed from blue to a blackish deep red. It was then stirred at 1100 rpm at room temperature under an air atmosphere for about 24 h. Note that the high-concentration synthesis (up to 0.6 M Cu salt) of AmIP Cu NPs was possible using the above synthetic method with no change to the mole ratio (Cu salt/AmIP/hydrazine = 1:10:10).

Purification. After the above reaction for around 24 h, the AmIP-Cu NPs were precipitated by adding excess *N,N*-dimethylacetamide into the colloidal dispersion of the Cu NPs, and the precipitates were washed with toluene and then hexane. Typically, 12 mL of the as-prepared colloidal dispersion of AmIP-Cu NPs was slowly added dropwise into 36 mL of *N,N*-dimethylacetamide solution, and the mixture became turbid due to the aggregation of AmIP-Cu NPs. The precipitates of AmIP-Cu NPs were obtained by centrifugation of the turbid solution for 5 min at 6000 rpm, as shown in Scheme 1. After the removal of the supernatant, the precipitate was washed again with 7 mL of *N,N*-dimethylacetamide, and then 10 mL of toluene and 10 mL hexane. In the washing process, the excess AmIP and hydrazine reagents were removed. After washing with hexane, the precipitates were at once used for the preparation of Cu nanoink for the analysis. Finally, purified AmIP-Cu NPs, with approximately 0.85 g of Cu content, were obtained from 2.73 g of copper acetate source. This corresponded to a reaction yield of about 90% and indicated the high recovery rate of Cu NPs from the synthesis and purification process.

Note that the selection of solvents in the above precipitation/washing process was very important to obtain a purified AmIP-Cu NP powder with high Cu content. If acetone was used as the precipitating/washing agent to form the colloidal dispersion of Cu NPs, the resulting powder was unstable; the powder could not be redispersed in solvents, and the oxidation of Cu NPs immediately occurred under an air atmosphere because of the removal of protecting AmIP layers from the surface of the AmIP-Cu NPs.

Cu Nanoink. Purified powders of AmIP-Cu NPs thus obtained were well-redispersed in propylene glycol/glycerol solvent (1:1 vol %) as Cu nanoink (~45 wt % Cu). The resultant Cu nanoink was kept in a freezer before use, and was stable for at least two months; no change in the resistivity of Cu conductive film made from the Cu nanoink was seen even after two months from the preparation of the nanoink. Actually, the oxidation of Cu NPs was minor even after the prolonged time of four months from the preparation of the nanoink, as shown in the XRD pattern of Cu nanoink (Figure S1 in Supporting Information, SI). The resistivity of the Cu film from the preparation of the nanoink at the heating of 150 °C after four months was about 80 $\mu\Omega$ cm, which had tripled compared to the case (~30 μ Ω cm) just after the preparation.

The Cu nanoink was applied to a polyimide film with a bar coater, and was dried at 80 °C for 60 min under a N_2 gas flow of 1.1 L/min. Then, the Cu film was sintered at various heating temperatures for 15 min in an electric furnace (FT-6000, FuLL-TECH, Osaka, Japan) under the N_2 gas flow. The thickness of the Cu film after heating was determined by surface roughness measurement instruments (SJ 310 Mitutoyo, Kanagawa, Japan) and the average thickness of the film calculated (~3 μm). The electrical resistivity of the Cu conductive film was analyzed using a four point probe (Loresta AX MCP-T370, Mitsubishi Chemical Analytech Co., Japan). To enhance the adhesion strength between the Cu film and the PET film, ultraviolet-ozone (UVO) oxidation (SSP16-110 Sen Lights Corp. Osaka, Japan) was

DOI: 10.1021/acsami.5b05542
ACS Appl. Mater. Interfaces 2015, 7, 19382−19389

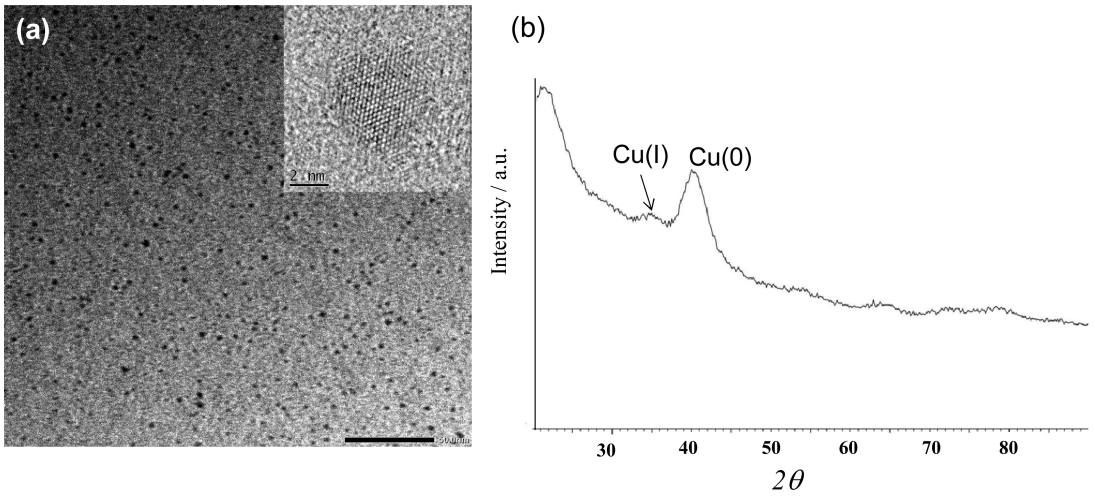

Figure 1. (a) TEM image of AmIP-Cu NPs. The high-magnification image is shown as the inset and illustrates that the crystal lattice fringes are 0.2 nm apart, which agrees with the *d* value of the (111) planes of the metallic Cu crystal. (b) XRD pattern for purified AmIP-Cu NPs.

performed on the PET film for 20 min. The luminous power of a low-pressure UV lamp was 15 mW/cm^2 at 254 nm under the UV irradiance at the distance of 30 mm.

2.3. Characterization. Fourier transform infrared spectroscopy (FT-IR) spectroscopy was performed using a Jasco FT-IR 4200 spectrometer coupled with an attenuated total reflection (ATR) instrument with a ZnSe crystal. X-ray photoelectron spectroscopy (XPS) spectra were recorded with a Quantera SXM spectrometer (Physical Electronics, Inc.) using the monochromatic Al Kα line at 1486.7 eV. The base pressure was approximately 2×10^{-8} Torr. To compensate for the charging effect, binding energies were referenced to C 1s at 284.7 eV of hydrocarbon. Transmission electron microscopy (TEM) images were recorded with a JEOL JEM-2010F at an acceleration voltage of 200 kV. Field emission scanning electron microscope (FE-SEM) images were collected on a JEOL model JSM-6700 FE-SEM operating at an accelerating voltage of 5.0 kV. X-ray diffraction (XRD) patterns were obtained on a Bruker D2 Phaser X-ray diffractometer (Cu Kα, λ = 1.5406 Å). Thermogravimetric analysis (TGA) was performed using a Thermo plus EVO device (Rigaku, Japan) at a heating rate of 10 °C/min under nitrogen flow. The initial viscosity of Cu nanoink (40 wt % Cu) was measured using a RST Plus Controlled Stress Rheometer (RST-CPS, Brookfield). The viscosity of Cu nanoink was 1350 mPa.

3. RESULTS AND DISCUSSION

3.1. Characterization of AmIP-Cu NPs. Figure 1a shows TEM images of AmIP-Cu NPs, which were obtained by the redispersion of purified AmIP-Cu NP powder in ethanol. The AmIP-Cu NPs had a narrow size distribution of 3.5 ± 1.0 nm, and they were well-dispersed. The size distribution diagram of Cu NPs is shown in Figure S2 in SI. The high-resolution (HR)-TEM image of the Cu NPs displays a periodic arrangement of stripes with a lattice spacing of 0.21 nm, which agrees with the (111) lattice spacing of fcc copper (Figure 1a, inset). The TEM observation proves that as-prepared AmIP-Cu NPs mainly comprise metallic Cu. Figure 1b shows the XRD pattern of AmIP-Cu NPs. A main diffraction peak emerges at 2θ angles of 40°−50°, which can be assigned to copper metal, Cu(0). The weak shoulder peak at 2θ angles around 35° may be attributed to Cu_2O obtained from Cu surface oxidation, Cu(I). The width of the diffraction peak is very large, which made it infeasible to estimate the particle size based on the Scherrer equation. The extreme width also indicates that as-prepared AmIP-stabilized Cu NPs have a very small particle size, which is consistent with the size estimation of approximately 3 nm in the corresponding TEM images.

Figure 2a shows an XPS spectrum of the Cu 2p region of the AmIP-Cu NPs. The characteristic peak of Cu 2p emerges at

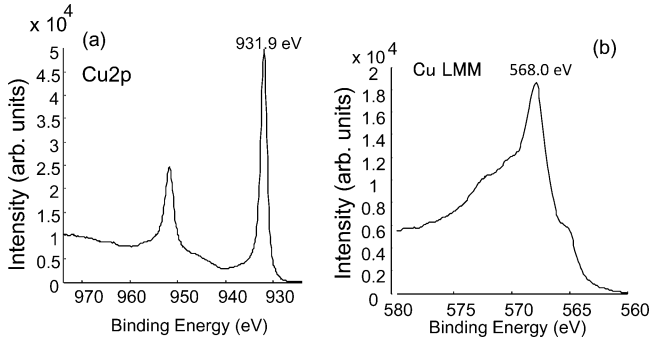

Figure 2. (a) XPS spectrum of AmIP-Cu NPs. (b) Cu-LMM AES spectrum for AmIP-Cu NPs.

931.9 eV, which is predominantly attributed to zero-valence copper, and is consistent with the peak obtained in a previous report which was attributed to zero-valence Cu crystals of approximately 2 nm in size.[35,36] A peak (~934 eV) associated with CuO obtained from surface oxidation was not observed in the AmIP-Cu NPs. The Auger electron spectroscopy (AES) of the AmIP-Cu NPs indicated the presence of zero-valence copper but the Cu-LMM peak lacked symmetry (Figure 2b), suggesting a mixture of Cu(0) and Cu(I) on the surface of AmIP-Cu NPs. From the above results of XRD and XPS spectra, we conclude that AmIP-Cu NPs comprise a main component of Cu(0) in the metallic core, and a minor component of Cu(I) on the surface. The results of XRD and XPS spectra showing the partial surface oxidation were different from the TEM image with the lattice spacing of fcc copper. This difference can be the different preparation sample method. The powder sample for XRD and XPS was obtained by drying under aerially exposed condition, while that for TEM was obtained by drying under high vacuum of the TEM instrument. Thus, we consider that the partial surface oxidation of Cu NPs occurred at the aerially exposed process in XRD and XPS. Note that the diffraction peak of Cu_2O in partially oxidized AmIP-Cu

DOI: 10.1021/acsami.5b05542
ACS Appl. Mater. Interfaces 2015, 7, 19382−19389

NPs, which is observed in the AmIP-Cu NPs before heat treatment, disappeared after heat treatment at 150 °C under a N_2 atmosphere. The reason for this reduction of Cu(I) to Cu(0) is the intrinsic reducing capacity of AmIP ligands, as discussed in detail later.

The IR spectra of free AmIP and AmIP-Cu NPs were acquired to clarify the presence of AmIP protective layers on the surface of the Cu NPs. Figure 3a shows the ATR-IR spectra

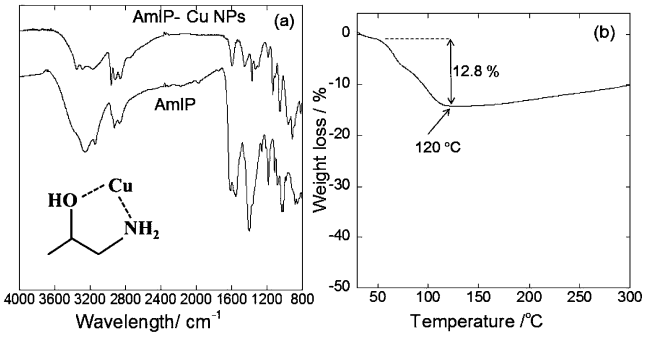

Figure 3. (a) ATR-IR spectra of AmIP-Cu NPs and Am-IP. A schematic of the metallacyclic coordination stability of a five-membered ring type between Cu and AmIP is shown as the inset. (b) TGA curve of Am-IP Cu NPs at a heating rate of 10 °C/min under a N_2 flow.

of free AmIP and AmIP-Cu NPs in the range 800−4000 cm^{-1}. Similar to the IR spectrum of free AmIP, the IR spectrum of AmIP-Cu NPs also covers an absorption band at 2850−2950 cm^{-1} from C−H stretch vibration of CH_3 and CH_2, and O−H and N−H stretch vibration in the range 3100−3400 cm^{-1}. These IR spectra of AmIP-Cu NPs confirm that Cu NPs are protected by AmIP molecules. The difference in N−H stretch vibration (3100−3400 cm^{-1}) and N−H vending (1550−1650 cm^{-1}) bands between the AmIP-Cu NPs and the free AmIP suggests the coordination of the amino groups of the AmIP to the surface of the Cu NPs.

In general, the use of strongly bonded organic stabilizers is a trade-off between the high-concentration synthesis of sub-10-nm Cu NPs and the undesirable presence of insulating organic stabilizers in the Cu film after thermal sintering of Cu nanoink, as mentioned above. Previously, we reported the synthesis of 2 nm Cu NPs via a microwave-assisted polyol method.[35] In this study, we conducted TGA analysis of the 2 nm Cu NPs, showing that the large amount of strongly bonded organic layers remained on the surface of the Cu NPs and were not removed even at high temperatures of ∼300 °C (Figure S3 in SI). These residual insulating materials displayed a high electrical resistivity (∼10^4 Ω cm) in the Cu film on the glass plate after heating at 200 °C for 60 min under a N_2 atmosphere (not shown). In contrast, we found that the AmIP ligands can be easily removed from the AmIP-Cu NPs at lower temperatures. The TGA analysis of purified AmIP-Cu NP powder demonstrated that elimination of the AmIP ligands from the Cu NPs was completed at low temperature (120 °C), as shown in Figure 3b. The amount of AmIP ligands on the Cu NPs can be estimated, from the TGA analysis, as 12.8%, indicating a very high Cu content of the purified AmIP-Cu NP powder. The elimination of the AmIP stabilizers from the Cu NPs at low temperature was also supported by the ATR-IR spectrum of the Cu film after heating at 150 °C, where there was no observation of IR peaks from the residual materials such as AmIP molecules and other organic molecules on the Cu surface (Figure S4 in SI).

Note that the gradual increase in the TGA curve above 200 °C is attributed to the oxidation of the Cu NPs, where the AmIP molecules are removed from the particle surface at the high temperatures, resulting in the enhancement of oxidation of the Cu NPs. The result demonstrates the importance of low heating temperatures (less than 200 °C) for producing conductive Cu film to avoid the oxidation of Cu NPs.

3.2. Optimization of the High-Concentration Synthesis of sub-10-nm AmIP-Cu NPs. In the high-concentration synthesis of sub-10-nm AmIP-Cu NPs developed in this study, the synthetic conditions were optimized for the stabilizers, solvent, reducing agents, and copper salt.

The AmIP stabilizer was selected to aid dissolution of a high concentration of copper(II) salt in ethylene glycol by complex formation of Cu(II)-AmIP, and to reduce the aggregation of Cu NPs by the adsorption of AmIP onto the nanoparticle surface. The amino group could coordinate with the copper ion or Cu NPs.

The combined use of hydrazine, copper(II) acetate, and ethylene glycol were important to achieve the high-concentration synthesis of sub-10-nm Cu NPs in this synthesis. For example, large aggregates of Cu NPs were formed when we used copper(II) formate as the replacement for copper(II) acetate in the synthesis (not shown), although copper(II) formate has been often used for the synthesis of Cu NPs due to the volatile and self-reducing properties of formate anions.[37−39] Propylene glycol is well-known as a typical polyol solvent,[40] but large aggregates of Cu NPs were formed when we used propylene glycol as the replacement for ethylene glycol in the synthesis (not shown).

In the colloid chemistry, it is known that fast nucleation relative to growth results in small particle size, depending on the concentration of reducing agents. Actually, the addition rate of hydrazine in the synthesis dramatically affected the resulting size of AmIP-Cu NPs. In synthesis A, hydrazine was added on only one occasion to the precursor Cu salt solution, producing very small AmIP-Cu NPs, as shown in Figure 1a. Synthesis B was conducted by the slow dropwise addition of hydrazine at a rate of ∼8 μL/s into the Cu salt solution, while maintaining the overall concentration and total volume of the reaction mixture constant. In synthesis B, larger Cu NPs of 5.5 ± 1.5 nm were obtained (Figure S5b in SI). The slow addition protocol likely enabled seed formation, followed by the controlled growth of the seeds into larger Cu NPs. Synthesis C was conducted using an even slower hydrazine addition rate of ∼24 μL/s to the Cu salt solution. In synthesis C, large and polydispersed AmIP-Cu NPs were precipitated (Figure S5c in SI). Therefore, the fast reduction of Cu salt by a one-time addition of hydrazine is necessary for the production of very small Cu NPs.

The most important factor in the synthesis of the Cu NPs was the use of 1-amino-2-propanol (AmIP) as the stabilizer. For comparison, 3-amino-1-propanol (AmNP) was also used in place of AmIP in the synthesis of Cu NPs. The AmNP is an isomer of Am IP: AmNP has a primary OH group, whereas AmIP has a secondary OH group. Interestingly, the use of AmNP produced larger, polydispersed Cu NPs with sizes 10−200 nm (Figure S6 in SI), in spite of synthetic conditions identical to those of AmIP-Cu NPs. This difference is probably due to the higher binding force of AmIP (when compared to that of Am NP) to the Cu nanoparticle surface, resulting in superior stability of the AmIP-Cu NPs. From the viewpoint of

DOI: 10.1021/acsami.5b05542
ACS Appl. Mater. Interfaces 2015, 7, 19382−19389

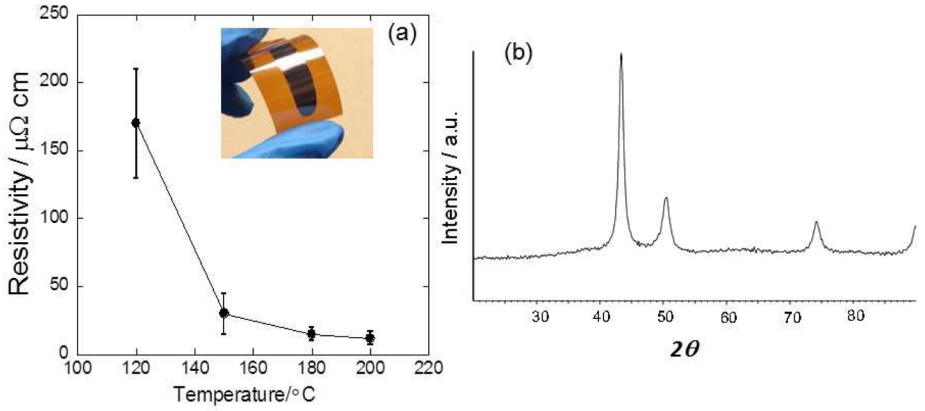

Figure 4. (a) Electrical resistivity of Cu film after the thermal sintering of Cu nanoink (45 wt % Cu, propylene glycol/glycerol solvent [1:1 vol %]) on polyimide film for 15 min at 120, 150, 180, and 200 °C. (b) XRD pattern for Cu film after the thermal sintering of Cu nanoink (45 wt % Cu, propylene glycol/glycerol solvent [1:1 vol %]) on polyimide film for 15 min at 150 °C.

geometric factors, the metallacyclic coordination stability of a five-membered ring type between Cu and AmIP is proposed for this higher binding force of AmIP onto the Cu surface (Figure 3a insert). The metallacyclic coordination stability of a five-membered ring type between the metal ion and the organic ligand is known in the coordination chemistry field.[41,42] Such metallacyclic coordination stability is not possible for the AmNP-Cu NPs due to the linear chemical structure of AmNP, resulting in larger, poly dispersed Cu NPs.

3.3. Thermal and Electrical Resistivity of Copper Conductive film. We measured the electrical resistivity of the Cu films prepared from the AmIP-Cu ink (45 wt % Cu) as a function of heating temperature from 85 to 200 °C for a short heating time of 15 min under a N_2 gas flow of 1.1 L/min.

The electrical resistivity of the Cu films at 85 °C was to be ~200 Ω, but it dramatically decreased to be ~170 μΩ at 120 °C (Figure 4a), most likely because of the removal of AmIP molecules from the particle surface and the sintering of the Cu NPs. The significant decrease in the electrical resistivity of the Cu film above 120 °C is consistent with the removal of AmIP molecules from the particle surface above 120 °C in the TGA curve (Figure 3b). A gradual decrease in electrical resistivity continued as the heating temperatures increased up to 200 °C. In a comparison with other reported Cu conductive inks, a low resistivity (~30 μΩ cm) occurred at a low temperature (150 °C). Figure 5a–f shows FE-SEM images of the morphology of the Cu films. Above a heating temperature of 120 °C, the Cu film showed sintering of the Cu NPs and particle size growth from about 3 nm to 50–100 nm, where the electrical resistivity of the Cu films dramatically decreased, as shown in Figure 4a. Furthermore, a gradual variation in the film morphology was observed as the heating temperature increased from 120 to 200 °C.

Note that a further decrease in the resistivity of the Cu films was observed when the thermal sintering period was prolonged from 15 to 60 min at a heating temperature of 120 °C, reducing the resistivity from 170 to 45 μΩ cm. A low heating temperature (120 °C) of Cu nanoink has the advantage for the production of conductive Cu film on flexible (polymeric) substrates with a low softening point (Tg) since the Tg of typical polymeric substrates, such as PET or polycarbonate (PC), is below 150 °C.

In contrast to the broad diffraction peaks observed before heating (Figure 1b), the XRD pattern of the Cu film after heating to 150 °C showed sharp diffraction peaks due to the growth size of the Cu NPs (Figure 4b). Interestingly, the diffraction peak of Cu_2O in partially oxidized AmIP-Cu NPs, which is observed in the AmIP-Cu NPs before the heat treatment (Figure 1b), disappeared after heat treatment at 150 °C under a N_2 atmosphere despite the absence of a reducing character gas such as hydrogen or formic acid. We consider that the secondary OH group of AmIP has the ability to reduce the Cu(I) to Cu(0) during the thermal sintering process of Cu NPs. In fact, we confirmed that the AmIP can in part reduce Cu_2O powder to metallic copper after heat treatment at 150 °C for 30 min under a N_2 atmosphere (Figure S7 in SI). Such a reduction of Cu_2O powder to metallic Cu was not observed for the use of AmNP or propylene glycol (not shown).

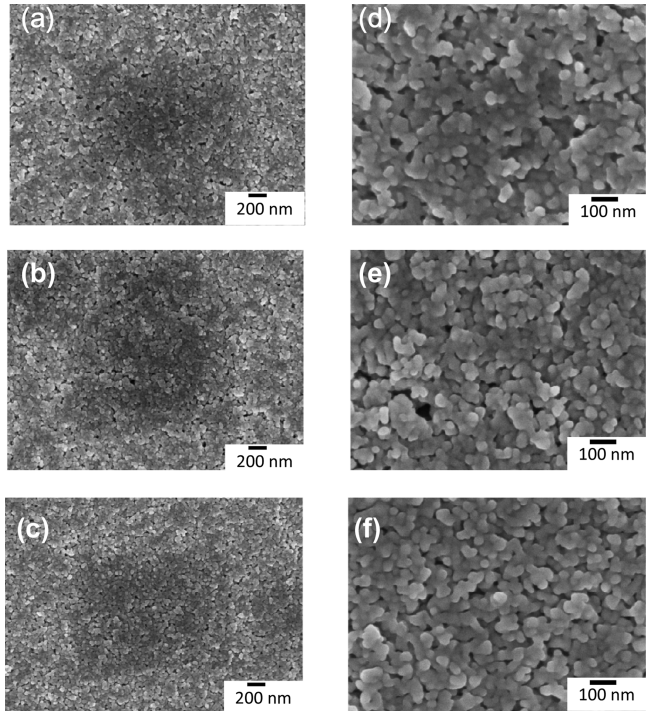

Figure 5. FE-SEM images of Cu film after the thermal sintering of Cu nanoink (45 wt % Cu, propylene glycol/glycerol solvent [1:1 vol %]) on polyimide film for 15 min at (a and d) 120, (b and e) 150, and (c and f) 200 °C at (a–c) ×30 000 and (d–f) ×100 000.

DOI: 10.1021/acsami.5b05542
ACS Appl. Mater. Interfaces 2015, 7, 19382–19389

Note that secondary alcohol from AmIP is also important in the low-heat removal of AmIP ligands from Cu NPs, resulting in the low electrical resistivity of Cu film because the secondary alcohols are oxidized to ketones during the heating, and the ketone products can be easily removed by heating due to their low boiling points. This is in contrast to the primary alcohol of Am NP, which is oxidized to either aldehydes or carboxylic acids with higher boiling points. The side reaction of aldehydes or carboxylic acids during heating may produce flameproof products of low electrical conductivity.

To confirm how the difference between the secondary alcohol of AmIP and primary alcohol of AmNP influences thermal elimination properties, AmNP-Cu NPs of size 5.8 ± 1.0 nm were newly synthesized in this study (Figure S8a in SI). Note that the same synthetic conditions as those of the AmIP Cu NPs produced AmNP-Cu NPs with large size, as described before (Figure S6 in SI). Therefore, we modified the synthetic procedure to obtain single nanosized AmIP Cu NPs (detailed synthetic method shown in Figure S8 in SI). The TGA analysis of purified AmIP Cu NPs showed the amount of AmNP to be about 13.5%, which is almost the same as that of AmIP-Cu NPs. However, TGA analysis showed that high-temperature heating (~250 °C) above the boiling point (~185 °C) of Am NP was necessary to eliminate the AmIP ligands from the Cu NPs (TG-DTA, Figure S8b in SI), and organic compounds remained in the higher heat conditions (~150 °C) (ATR-IR, Figure S8c in SI), in contrast to the lower heat (~120 °C) removal of AmIP from the Cu NPs. As a result, the Cu film from the AmNP-Cu conductive ink (40 wt % Cu, propylene glycol/glycerol solvent [1:1 vol %]) showed very high resistivity (~10^4 Ω cm) due to the presence of flameproof products, although metallic Cu without oxidation was observed in the XRD spectrum (Figure 8d in SI). This is because the organic stabilizers remain as insulating organic shells around each Cu particle surface after the thermal sintering of Cu nanoink at a low temperature (180 °C), leading to the prevention of electrical conductivity in the Cu film.

Long-term low resistance of Cu film under air exposure is necessary for practical applications. Figure 6 shows the time-dependent resistance of Cu film after heating at 150, 180, and 200 °C as a function of air exposure time at room temperature and humidity (23 ± 2 °C and 30% ± 5%, respectively). The values of resistivity were normalized to the resistivity value immediately after the heat treatment. The resistance gradually increased with time. This is probably because of the formation of Cu oxide on the Cu film surface under air exposure. The resistance showed a rapid increase within the first day of air exposure, and then increased by slow degrees. After around 4 months, the resistance increased by 1.7, 1.4, and 1.2 times (relative to that of the as-prepared Cu film) for the heating temperatures 150, 180, and 200 °C, respectively. Nevertheless, the resistance of the Cu film remained around 10^{-5} Ω cm even after air exposure of about 4 months, indicating the long-term low resistance of Cu film under air exposure.

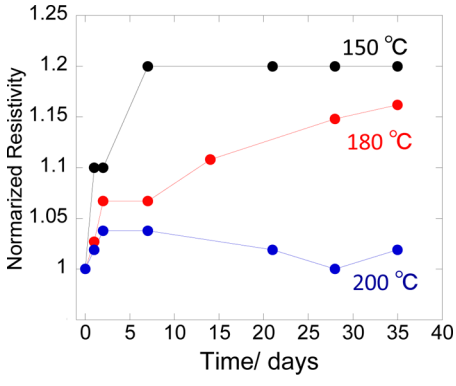

Figure 6. Time-dependent resistance of Cu film on polyimide film after different heat treatments at 150, 180, and 200 °C as a function of air exposure time at 23 °C and 30 ± 5% humidity.

Note that the increase of Cu film resistance with time was smaller for the film heated at higher temperature. This difference is likely due to the larger growth size and sintering of Cu NPs at higher temperature. The insufficient sintering of Cu NPs at 150 °C facilitates the formation of Cu oxides resulting in the fast increase of Cu film resistance with time, while the sufficient sintering of Cu NPs at 200 °C suppresses the formation of Cu oxides under air exposure. At the intermediate sintering temperature of 180 °C, the formation of Cu oxides proceeds slowly (i.e., slow increase of resistance with time) compared to the case at 150 °C.

A further concern for the manufactures of printed circuitry is to ensure adhesion to a chosen substrate. Once the ink loses its adhesion, it can fail in its intended purpose to transmit electrical current. A cross cut test (i.e., a measure of adhesion strength) is one method for determining the resistance of paints and coatings to their separation from substrates.[43] This test uses a tool to cut a right angle lattice pattern into the coating. In this study, triple cross cut tests were conducted for the Cu film on PET film. The Cu film on PET film was prepared by the thermal sintering of Cu nanoink (45 wt % Cu, propylene glycol/glycerol solvent [1:1 vol %]) at 150 °C. In general, the Cu nanoink contains binder polymers, such as epoxy resin and ethylcellulose, to increase the adhesion strength on the substrate. However, there is fear that the use of such binders increases the resistivity of Cu film due to the flameproof binder products, notably in low-heat sintering below 150 °C. In place of binder polymers, therefore, UVO oxidation of PET surfaces was utilized to increase the adhesion strength of Cu film on the PET film in this study.

As shown in Figure 7a, the Cu film on nontreated PET film showed very poor adhesion to the substrate in the cross cut test, despite a low resistance of 25 μΩ cm. Most of the Cu film on the PET flaked in the first cross cut test. This is because the Cu nanoink contains no binder polymers. In contrast, adhesion strength dramatically increased in the case of Cu film on UVO-treated PET film. Even after the third cross cut test, the Cu film flaked only along the edges and/or at the intersections of the

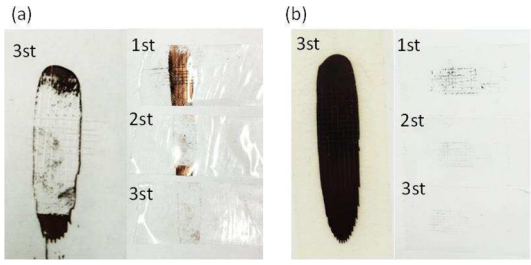

Figure 7. Adhesion strength tests of the Cu film on (a) nontreated PET and (b) UVO-treated PET prepared by the thermal sintering of Cu nanoink (45 wt % Cu, propylene glycol/glycerol solvent [1:1 vol %]) for 15 min at the temperature of 150 °C. The triple cross cut test was conducted for the Cu film on these PET films.

DOI: 10.1021/acsami.5b05542
ACS Appl. Mater. Interfaces 2015, 7, 19382−19389

cuts, indicating greater adhesion strength (Figure 7b). In addition, the electrical resistivity of the Cu film did not change appreciably for both the PET and oxidized PET substrates. It has been reported that UVO treatment on a PET film produces oxidized surfaces rich in COOH/COOR.[44] It is most likely that these polar species on oxidized PET increased the adhesion strength between AmIP-Cu NPs and the PET via the interaction with amino ($-NH_2$) and hydroxyl ($-OH$) groups of AmIP ligands. We did not notice any alteration of mechanical properties such as flexibility and fragility of PET film. On the other hand, the oxidized surfaces after UVO treatment provided a substantial improvement in the wettability of PET film for the ink solvent of propylene glycol/glycerol solvent (1:1 vol %). In addition, slightly yellow PET film was observed. The UVO treatment on the PET not only enhanced the adhesion strength but also maintained the low electrical resistance for AmIP-based Cu nanoinks.

CONCLUSION

A simple, high-concentration (up to 0.6 M Cu salt) synthesis of sub-10-nm Cu NPs was developed in ethylene glycol at room temperature under ambient air conditions, using AmIP as the stabilizer and hydrazine monohydrate as the reducing agent. Monodispersed spherical AmIP-Cu NPs of 3.5 ± 1.0 nm were synthesized in about 90% yield. Thus, nearly 1 g of sub-10-nm Cu NP powder was obtained by one-step synthesis for the first time. It was proposed that metallacyclic coordination stability of a five-membered ring type between Cu and AmIP contributed to this higher binding force of AmIP onto the Cu surface, resulting in the superior stability and single nanosize of the AmIP-Cu NPs.

The purified AmIP-Cu NP powder could be redispersed in alcohol-based solvents such as ethanol and propylene glycol up to high Cu contents of 45 wt %. Conductive copper films were obtained by depositing the Cu nanoink on polyimide film, and the resistivity of the conductive copper film was 30 $\mu\Omega$ cm after thermal heating at 150 °C for 15 min under a nitrogen flow. We experimentally proved that AmIP can be effective as the reducing agent for Cu_2O to metallic copper in the thermal annealing process.

In relation to the potential application in the printed electronics industry, the long-term resistance stability of Cu film under an air atmosphere was determined, and an adhesion test on PET film was conducted. A low resistance of the Cu film (10^{-5} Ω cm) was observed even after air exposure of around 4 months, and the air stability of the Cu film was better for the high-temperature treated film because of sufficient growth size and sintering of Cu NPs at higher sintering temperatures. The Cu film on PET film showed poor adhesion to the substrate in the cross cut test. In contrast, the adhesion strength dramatically increased in the case of Cu film on PET film oxidized by UVO treatment. The UVO treatment on the PET not only enhances the adhesion strength but also maintains low electrical resistance for AmIP-based Cu nanoinks.

ASSOCIATED CONTENT

Supporting Information

The Supporting Information is available free of charge on the ACS Publications website at DOI: 10.1021/acsami.5b05542.

XRD patterns, IR spectrum, size distribution diagram, TEM images, TGA data (PDF)

AUTHOR INFORMATION

Corresponding Author

*E-mail: hkawa@kansai-u.ac.jp.

Notes

The authors declare no competing financial interest.

ACKNOWLEDGMENTS

We thank Prof. K. Suganuma and Dr. T. Sugahara at Osaka University for the thickness measurements of the Cu film and the helpful discussion about Cu nanoink. We also thank Ms. Yukiko Mori at Kansai University for the helpful discussion on the purification of Cu nanoink. This work was supported by JSPS KAKENHI (Grants 15H03520, 15H03526, and 26107719), and the Network Joint Research Center for Materials and Devices (2013A20).

REFERENCES

(1) Lee, Y.; Choi, J.-R.; Lee, K. J.; Stott, N. E.; Kim, D. Large-scale Synthesis of Copper Nanoparticles by Chemically Controlled Reduction for Applications of inkjet-printed electronics. *Nanotechnology* **2008**, *19*, 415604.

(2) Tanabe, K. Optical Radiation Efficiencies of Metal Nanoparticles for Optoelectronic Applications. *Mater. Lett.* **2007**, *61*, 4573−4575.

(3) Isomura, Y.; Narushima, T.; Kawasaki, H.; Yonezawa, T.; Obora, Y. Surfactant-free Single-nano-sized Colloidal Cu Nanoparticles for Use as an Active Catalyst in Ullmann-coupling Reaction. *Chem. Commun.* **2012**, *48*, 3784−3786.

(4) Ramyadevi, J.; Jeyasubramanian, K.; Marikani, A.; Rajakumar, G.; Rahuman, A. Synthesis and Antimicrobial Activity of Copper Nanoparticles. *Mater. Lett.* **2012**, *71*, 114−116.

(5) Magdassi, S.; Grouchko, M.; Kamyshny, A. Copper Nanoparticles for Printed Electronics: Routes Towards Achieving Oxidation Stability. *Materials* **2010**, *3*, 4626−4638.

(6) Lai, C. Y.; Cheong, C. F.; Mandeep, J. S.; Abdullah, H. B.; Amin, N.; Lai, K. W. Synthesis and Characterization of Silver Nanoparticles and Silver Inks: Review on the Past and Recent Technology Roadmaps. *J. Mater. Eng. Perform.* **2014**, *23*, 3541−3550.

(7) Jo, Y.; Oh, S. J.; Lee, S. S.; Seo, Y. H.; Ryu, B. H.; Moon, J.; Choi, Y.; Jeong, S. Extremely Flexible, Printable Ag Conductive Features on PET and Paper Substrates via Continuous Millisecond Photonic Sintering in a Large Area. *J. Mater. Chem. C* **2014**, *2*, 9746−9753.

(8) Ahn, Y.; Lee, H.; Lee, D.; Lee, Y. Highly Conductive and Flexible Silver Nanowire-Based Microelectrodes on Biocompatible Hydrogel. *ACS Appl. Mater. Interfaces* **2014**, *6*, 18401−18407.

(9) Kim, N. R.; Lee, H. M. Synthesis of Low-temperature-processable and Highly Conductive Ag Ink by a Simple Ligand Modification: the Role of Adsorption Energy. *J. Mater. Chem. C* **2013**, *1*, 1855−1862.

(10) Lee, Y.; Choi, J.r.; Lee, K. J.; Stott, N. E.; Kim, D. Large-scale Synthesis of Copper Nanoparticles by Chemically Controlled Reduction for Applications of Inkjet-printed Electronics. *Nanotechnology* **2008**, *19*, 415604.

(11) Kang, J. S.; Kim, H. S.; Ryu, J.; Hahn, H. T.; Jang, S.; Joung, J. W. Inkjet Printed Electronics using Copper Nanoparticle Ink. *J. Mater. Sci.: Mater. Electron.* **2010**, *21*, 1213−1220.

(12) Jianfeng, Y.; Guisheng, Z.; Anming, H.; Zhou, Y. N. Preparation of PVP coated Cu NPs and the Application for Low-temperature Bonding. *J. Mater. Chem.* **2011**, *21*, 15981−15986.

(13) Wang, B.; Chen, S.; Nie, J.; Zhu, X. Facile Method for Preparation of Superfine Copper Nanoparticles with High Concentration of Copper Chloride Through Photoreduction. *RSC Adv.* **2014**, *4*, 27381−27388.

(14) Wu, C. J.; Chen, S. M.; Sheng, Y. J.; Tsao, H. K. Anti-oxidative Copper Nanoparticles and Their Conductive Assembly Sintered at Room Temperature. *J. Taiwan Inst. Chem. Eng.* **2014**, *45*, 2719−2724.

(15) Qin, G.; Watanabe, A.; Tsukamoto, H.; Yonezawa, T. Copper Film Prepared from Copper Fine Particle Paste by Laser Sintering at

DOI: 10.1021/acsami.5b05542
ACS Appl. Mater. Interfaces 2015, 7, 19382−19389

Room Temperature: Influences of Sintering Atmosphere on the Morphology and Resistivity. *Jpn. J. Appl. Phys.* **2014**, *53*, 096501.
(16) Joo, S. J.; Park, S. H.; Moon, C. J.; Kim, H. S. A Highly Reliable Copper Nanowire/Nanoparticle Ink Pattern with High Conductivity on Flexible Substrate Prepared via a Flash Light-Sintering Technique. *ACS Appl. Mater. Interfaces* **2015**, *7*, 5674−5684.
(17) Woo, K.; Kim, Y.; Lee, B.; Kim, J.; Moon, J. Effect of Carboxylic Acid on Sintering of Inkjet-Printed Copper Nanoparticulate Films. *ACS Appl. Mater. Interfaces* **2011**, *3*, 2377−2382.
(18) Kim, C.; Lee, G.; Rhee, C.; Lee, M. Expeditious Low-temperature Sintering of Copper Nanoparticles with Thin Defective Carbon Shells. *Nanoscale* **2015**, *7*, 6627−6635.
(19) Yong, Y.; Yonezawa, T.; Matsubara, M.; Tsukamoto, H. The Mechanism of Alkylamine-stabilized Copper Fine Particles Towards Improving the Electrical Conductivity of Copper Films at Low Sintering Temperature. *J. Mater. Chem. C* **2015**, *3*, 5890−5895.
(20) Lignier, P.; Bellabarba, R.; Tooze, R. P. Scalable Strategies for the Synthesis of Well-defined Copper Metal and Oxide Nanocrystals. *Chem. Soc. Rev.* **2012**, *41*, 1708−1720.
(21) Yanase, A.; Komiyama, H. In Situ Observation of Oxidation and Reduction of Small Supported Copper Particles using Optical Absorption and X-ray Diffraction. *Surf. Sci.* **1991**, *248*, 11−19.
(22) Kanninen, P.; Johans, C.; Merta, J.; Kontturi, K. Influence of Ligand Structure on the Stability and Oxidation of Copper Nanoparticles. *J. Colloid Interface Sci.* **2008**, *318*, 88−95.
(23) Pacioni, N. L.; Filippenko, V.; Presseau, N.; Scaiano, J. C. Oxidation of Copper Nanoparticles in Water: Mechanistic Insights Revealed by Oxygen Uptake and Spectroscopic Methods. *Dalton Trans.* **2013**, *42*, 5832−5838.
(24) Wu, S. H.; Chen, D. H. Synthesis of High-concentration Cu Nanoparticles in Aqueous CTAB Solutions. *J. Colloid Interface Sci.* **2004**, *273*, 165−169.
(25) Nakamura, T.; Tsukahara, Y.; Sakata, T.; Mori, H.; Kanbe, Y.; Bessho, H.; Wada, Y. Preparation of Monodispersed Cu Nanoparticles by Microwave-Assisted Alcohol Reduction. *Bull. Chem. Soc. Jpn.* **2007**, *80*, 224−232.
(26) Yu, W.; Xie, H.; Chen, L.; Li, Y.; Zhang, C. Synthesis and Characterization of Monodispersed Copper Colloids in Polar Solvents. *Nanoscale Res. Lett.* **2009**, *4*, 465−470.
(27) Zhang, H. X.; Siegert, U.; Liu, R.; Cai, W. B. Facile Fabrication of Ultrafine Copper Nanoparticles in Organic Solvent. *Nanoscale Res. Lett.* **2009**, *4*, 705−708.
(28) Dadgostar, N.; Ferdous, S.; Henneke, D. Colloidal Synthesis of Copper Nanoparticles in a Two-phase Liquid−Liquid System. *Mater. Lett.* **2010**, *64*, 45−48.
(29) Huaman, J. L. C.; Sato, K.; Kurita, S.; Matsumoto, T.; Jeyadevan, B. Copper Nanoparticles Synthesized by Hydroxyl Ion Assisted Alcohol Reduction for Conducting Ink. *J. Mater. Chem.* **2011**, *21*, 7062−7069.
(30) Niranjan, M. K.; Chakraborty, J. Synthesis of Oxidation Resistant Copper Nanoparticles in Aqueous Phase and Efficient Phase Transfer of Particles Using Alkanethiol. *Colloids Surf., A* **2012**, *407*, 58−63.
(31) Choi, C. S.; Jo, Y. H.; Kim, M. G.; Lee, H. M. Control of Chemical Kinetics for Sub-10 nm Cu Nanoparticles to Fabricate Highly Conductive Ink below 150 °C. *Nanotechnology* **2012**, *23*, 065601.
(32) Deng, D.; Cheng, Y.; Jin, Y.; Qi, T.; Xiao, F. Antioxidative Effect of Lactic Acid-stabilized Copper Nanoparticles Prepared in Aqueous Solution. *J. Mater. Chem.* **2012**, *22*, 23989−23995.
(33) Yang, G.; Zhang, Z.; Zhang, S.; Yu, L.; Zhang, P. Synthesis and Characterization of Highly Stable Dispersions of Copper Nanoparticles by a Novel One-pot Method. *Mater. Res. Bull.* **2013**, *48*, 1716−1719.
(34) Chowdhury, P. P.; Shaik, A. H.; Chakraborty, J. Preparation of Stable Sub 10 nm Copper Nanopowders Redispersible Inpolar and Non-polar Solvents. *Colloids Surf., A* **2015**, *466*, 189−196.
(35) Kawasak, H.; Kosaka, Y.; Myoujin, Y.; Narushima, T.; Yonezawa, T.; Arakawa, R. Microwave-assisted Polyol Synthesis of Copper Nanocrystals Without using Additional Protective Agents. *Chem. Commun.* **2011**, *47*, 7740−7742.
(36) Brege, J. J.; Hamilton, C. E.; Crouse, C. A.; Barron, A. R. Ultrasmall Copper Nanoparticles from a Hydrophobically Immobilized Surfactant Template. *Nano Lett.* **2009**, *9*, 2239−2242.
(37) Yabuki, A.; Arriffin, N.; Yanase, M. Low-temperature Synthesis of Copper Conductive Film by Thermal Decomposition of Copper−amine Complexes. *Thin Solid Films* **2011**, *519*, 6530−6533.
(38) Kim, I.; Kim, Y.; Woo, K.; Ryu, E. H.; Yon, K. Y.; Cao, G.; Moon, J. Synthesis of Oxidation-resistant Core−shell Copper Nanoparticles. *RSC Adv.* **2013**, *3*, 15169−15177.
(39) Koyama, S.; Hagiwara, N.; Shohji, I. Cu/Cu Direct Bonding by Metal Salt Generation Bonding Technique with Organic Acid and Persistence of Reformed Layer. *Jpn. J. Appl. Phys.* **2015**, *54*, 030216.
(40) Carroll, K. J.; Reveles, J. U.; Shultz, M. D.; Khanna, S. N.; Carpenter, E. E. Preparation of Elemental Cu and Ni Nanoparticles by the Polyol Method: An Experimental and Theoretical Approach. *J. Phys. Chem. C* **2011**, *115*, 2656−2664.
(41) Omae, I. Three Types of Reactions with Intramolecular Five-membered Ring Compounds in Organic Synthesis. *J. Organomet. Chem.* **2007**, *692*, 2608−2632.
(42) Rosenthal, U.; Burlakov, V. V.; Bacha, M. A.; Beweries, T. Five-membered Metallacycles of Titanium and Zirconium − Attractive Compounds for Organometallic Chemistry and Catalysis. *Chem. Soc. Rev.* **2007**, *36*, 719−728.
(43) Kim, Y.; Lee, B.; Yang, S.; Byun, I.; Jeong, I.; Cho, S. M. Use of Copper Ink for Fabricating Conductive Electrodes and RFID Antenna Tags by Screen Printing. *Curr. Appl. Phys.* **2012**, *12*, 473−478.
(44) Ton-That, C.; Teare, D. O. H.; Campbell, T P. A.; Bradley, R. H. Surface Characterisation of Ultraviolet-ozone Treated PET using Atomic Force Microscopy and X-ray Photoelectron Spectroscopy. *Surf. Sci.* **1999**, *433*−*435*, 278−282.

DOI: 10.1021/acsami.5b05542
ACS Appl. Mater. Interfaces 2015, 7, 19382−19389